Dual-Readout Calorimetry for High-Quality Energy Measurements

Progress Report
and
Request for allocation of resources

Presented by:

Dr. Gabriella Gaudio and Dr. Richard Wigmans[1]

on behalf of the DREAM Collaboration

(Cagliari - Cosenza - Iowa State - Pavia - Pisa - Roma I - Texas Tech)

1 June 2011

[1]Contact person. Tel. [806] 742 3779, FAX [806] 742 1182, E-mail: wigmans@ttu.edu

1 Introduction

On April 13, 2010, the DREAM project was presented in an open session of the SPS Committee at CERN [1]. We discussed the need for improved hadron calorimetry in future experiments, the ideas on which the dual-readout approach is based, and showed results obtained during 7 years of beam tests of prototype calorimeters at the SPS. We also asked CERN to support our future plans, which include the construction of a full-scale fiber calorimeter that should expectedly set new records for the precision with which hadrons and jets can be measured.

This proposal was well received by the SPSC. As a result, we were offered a new experimental area, in the H8 beam line, where a permanent setup could be made, as well as a dedicated control room. With the help of Dr. Ilias Efthymiopoulos and Michael Jeckel this real estate has been adapted to our needs, and during the summer of 2010, the first measurements in our new experimental setup in H8 were carried out. Some results of these measurements have recently been published, namely

1. N. Akchurin *et al.*, *Polarization as a Tool for Dual-Readout Calorimetry*, Nucl. Instr. and Meth. **A638** (2011) 47 - 54.
2. N. Akchurin *et al.*, *A Comparison of BGO and BSO Crystals Used in the Dual-Readout Mode*, Nucl. Instr. and Meth. **A640** (2011) 91 - 98.

In this report, we summarize new experimental results obtained in the past year, progress towards the construction of the new detector(s), as well as our near- and long-term plans. We also want to ask the SPSC to recognize this project as an integral part of the CERN experimental program by assigning an RD project number to it. Even though this might seem a formality, it may have important practical implications.

2 DREAM Calorimeter R&D for Future Experiments

2.1 Recent results with crystals

Once the effects of fluctuations in the em shower fraction $f_{\rm em}$ are eliminated, which is the purpose of the dual-readout method, the energy resolution of a DREAM calorimeter is dominated by other factors, and in particular by sampling fluctuations and fluctuations in the number of signal quanta in the Čerenkov channel. Of course, if the detector is not large enough to contain the showers, then leakage fluctuations will also play an important role, but this problem can be trivially solved by making the instrument sufficiently large.

In order to address these newly dominating factors, an important part of our experimental program in the past couple of years has concentrated on using high-Z crystals instead of fibers. If successful, both sampling fluctuations and fluctuations resulting from the limited Čerenkov light yield could be made negligibly small in that case. The challenge is then to extract separate scintillation and Čerenkov signals from the light generated by showers developing in these crystals. We have found four different ways to do this, using a) the directionality, b) spectral differences, c) the time structure and d) the polarization of the signals. Figure 1 illustrates the first three of the mentioned methods. The experimental data were obtained with molydenum-doped lead tungstate crystals, which were custom made for our project. The purpose of the (0.3%) Mo doping is to increase the decay time of the scintillation process in the $PbWO_4$ crystal (from $\sim$10 to $\sim$30 ns), and to shift the scintillation spectrum to somewhat longer wavelengths. As a result, with the proper optical transmission filters, it was possible to obtain almost pure signals of the Čerenkov and scintillation components of the light generated by developing showers in this crystal (method b, Figure 1b). The Čerenkov nature of the light transmitted by the UV filter mounted on side R of the crystal (Figure 1a) is illustrated by the prompt time structure of the signals, as opposed to the characteristic decay time of the scintillation light transmitted by the yellow filter (method c, Figure 1b). The directionality of the Čerenkov component (method a) is illustrated by the characteristic dependence of the ratio of the two signals on the angle of incidence of the beam particles (Figure 1a,c). This ratio peaks at $\theta = 27°$, at which angle the Čerenkov cone impinges perpendicular onto the PMT intended for the detection of Čerenkov light, thus maximizing the acceptance.

The latter geometry is also shown in Figure 2a, which depicts the Čerenkov cone as well.

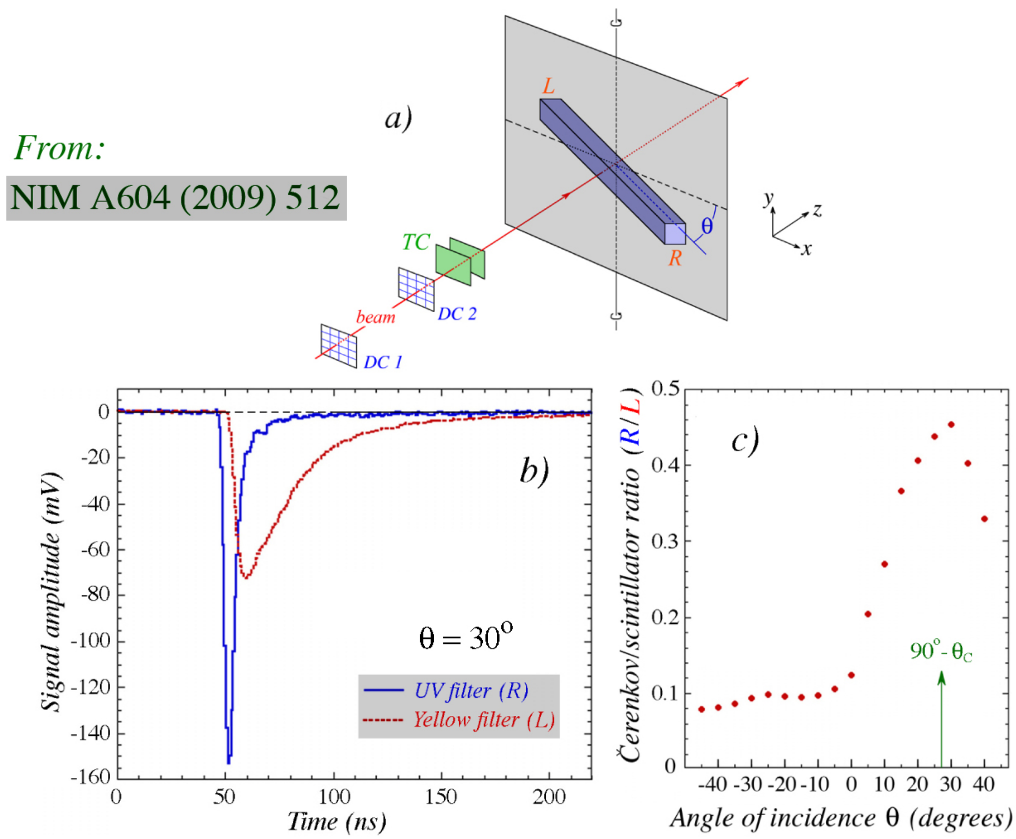

Figure 1: Unraveling of the signals from a Mo-doped $PbWO_4$ crystal into Čerenkov and scintillation components. The experimental setup is shown in diagram a. The two sides of the crystal were equipped with a UV filter (side R) and a yellow filter (side L), respectively. The time structure of the R and L signals from 50 GeV electrons traversing the crystal is shown in diagram b and the angular dependence of the ratio of these two signals is shown in diagram c [2].

This figure is intended to illustrate the fourth method mentioned above, in which the two types of light are distinguished on the basis of the fact that the Čerenkov light is polarized. The direction of the polarization vector of the light cone that strikes the end face of the crystal is indicated in Figure 2b. These measurements were performed with a crystal of BSO (bismuth silicate), which has the same crystal structure as BGO ($Bi_4Si_3O_{12}$), with silicon atoms replacing the germanium ones. Figures 2c,d show the time structures of the signals from this crystal using the same optical transmission filters as in Figure 1. Also in this case, these filters achieve a good separation between the (prompt) Čerenkov and long-lived (100 ns decay time) scintillation light, albeit that the UV signal clearly contains some significant contamination from the scintillation component. However, the essence of this figure is contained in diagrams e, f, which show the time structure of the UV component for two orientations of the polarization filter that was installed in between the optical transmission filter and the PMT. The fact that the prompt Čerenkov component almost completely disappears when the transmission axis of the polarization crystal is rotated from horizontal (see diagram b) to vertical, while the contaminating scintillation component is unaf-

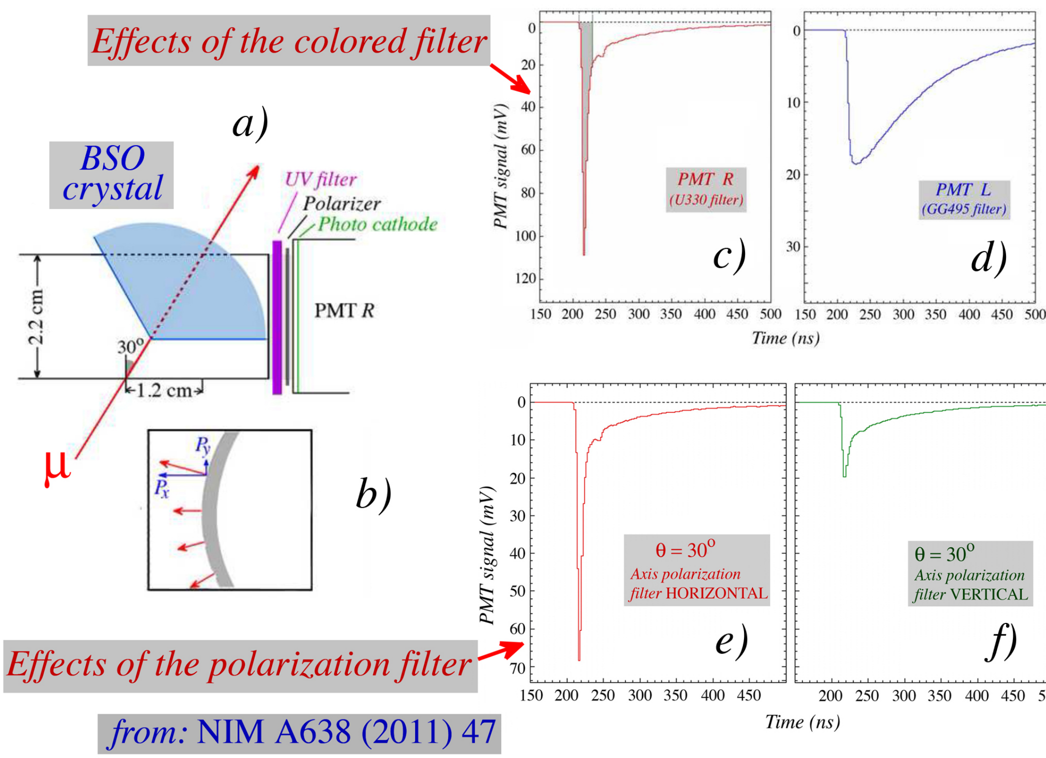

Figure 2: Polarization as a tool to distinguish Čerenkov and scintillation light. Emission of Čerenkov light by particles traversing the BSO crystal at $\theta = 30°$. Shown are a top view (a) and a view from the end face from which the Čerenkov photons exit the crystal (b). The Čerenkov cone is indicated by the shaded area in a, and the polarization vectors of the detected Čerenkov photons by the arrows in b. The other diagrams show the average time structure of the signals generated by 180 GeV π^+ traversing this crystal in its center at $\theta = 30°$ and passing through different filters, as indicated in a. The UV filter selects predominantly Čerenkov light (c), as opposed to a yellow filter mounted on the other end of the crystal, which transmits almost exclusively scintillation light (d). The transmission axis of the polarization filter is either oriented horizontally (e) or vertically (f), illustrating the high degree of polarization of the Čerenkov light.

fected by this operation, illustrates the high degree of polarization of the Čerenkov component of the detected UV signals [3].

The properties of the BSO crystals turned out to be very interesting in their own right for the purpose of application as dual-readout calorimeters. We performed a separate study in which these properties were compared in detail with those of the more commonly used BGO crystals. One attractive feature, illustrated in Figure 2c, is the fact that by using a UV filter, information about both the scintillation and the Čerenkov component can be obtained from one signal, using the distinctly different time structures of these components. This feature was also successfully used when we tested a BGO matrix in conjunction with the fiber calorimeter [4]. However, in comparison with BGO, BSO offers several distinct advantages. In particular, it has a considerably higher Čerenkov light yield, and with a given UV filter the separation between the Čerenkov and scintillation signals is substantially better in this crystal [5]. These features, combined with the fact that no expensive components such as germanium are needed for the production, which may imply an important cost advantage, makes BSO a very interesting candidate for a homogeneous dual-readout calorimeter.

Measurements in which the original fiber module was preceded by a crystal matrix serving as the em calorimeter section offered similar possibilities to measure $f_{\rm em}$ event by event as measurements of the fiber module in stand-alone mode [6, 7].

2.2 The future: SuperDREAM

Even though the results obtained with crystals indicate that the dual-readout method makes it in principle possible to build excellent homogeneous (fully sensitive) hadron calorimeters, the DREAM Collaboration has at this point decided to concentrate mainly on the fiber option, for the following reasons:

1. The fact that neutron detection in the hydrogenous fibers provides a handle on fluctuations in nuclear binding energy losses that is not available for crystals

2. The fact that attenuation of the crucially important Čerenkov light is much less of a problem in fibers than in crystals

3. The enormous (and prohibitive) cost of building a crystal-based detector that is large enough to contain the showers induced by hadrons and jets at a sufficient level

Yet, even though we will dedicate our available resources primarily towards the construction of a new fiber calorimeter, tests of this detector in conjunction with a crystal matrix serving as the em calorimeter section will also be part of the experimental program. We would like to point out that such a hybrid system is probably the only way to obtain, in addition to excellent hadronic performance, also energy resolutions better than $5\%/\sqrt{E}$ for em showers.

Based on the results obtained in the past 8 years, we believe that we have all the elements in hand to design a calorimeter that will meet and exceed the requirements of ILC/CLIC experiments, and that will set new performance records for hadron calorimetry. This detector will be large enough to contain high-energy hadron showers at the 99% level, such as to eliminate the effects of leakage fluctuations, which dominated the energy resolution of the original one-ton fiber module. After fluctuations in em shower content are eliminated with the dual-readout method, the hadronic energy resolution of this fiber calorimeter is dominated by sampling fluctuations and fluctuations in Čerenkov light yield. We aim to reduce both sources of (Poisson) fluctuations to about $10\%/\sqrt{E}$. In that case, the hadronic energy resolution ($\sim 20\%/\sqrt{E}$) will approach the theoretical limit, while electrons and γs should be detected with resolutions better than $10\%/\sqrt{E}$. These improvements are achieved by making the following modifications to the original DREAM fiber module:

- Fibers are individually embedded in the absorber structure, instead of in groups of seven
- The packing fraction of the fibers is roughly doubled
- The numerical aperture of the Čerenkov fibers is increased
- The upstream end of the Čerenkov fibers is aluminized
- The quantum efficiency of the photocathode is increased (using Super Bialkali PMTs)

Another important difference with the original DREAM fiber calorimeter concerns the readout, which is based on a Domino Ring Sampler (DRS) circuit that allows time structure measurements of each signal with a sampling rate of 2.5 GHz (0.4 ns time resolution). Prototype versions of this chip were tested extensively by us during the past couple of years, and the results were such that CAEN decided to develop a commercial module based on this principle. This module has 16 channels, each of which allows time structure measurements with a resolution that was until now only achievable with top-of-the-line digital sampling oscilloscopes. We have shown previously that detailed measurements of the time structure are an invaluable source of information, not only for separating the Čerenkov and scintillation signals from crystals, but also to identify and measure the contribution of neutrons to the scintillation signals [8]. Another important goal of the time structure measurements is to determine the depth at which the light is produced in this longitudinally unsegmented calorimeter. To this end, we plan to make use of the fact that the light signals travel at a slower speed in the fibers ($\sim$ 17 cm/ns) than the particles producing this light (30 cm/ns). And finally, thanks to the aluminized upstream ends of the Čerenkov fibers, the time structure measurements will give us important additional tools to identify electrons in this unsegmented calorimeter (Figure 3).

Details of the proposed detector development program are described in [1].

3 Current and planned activities

3.1 Current activities

The collaboration has decided that the new fiber calorimeter will be constructed in Italy. The availability of adequate workshop facilities and the experience of several collaborators with building calorimeters of a similar type (KLOE, SPACAL) were important considerations in this

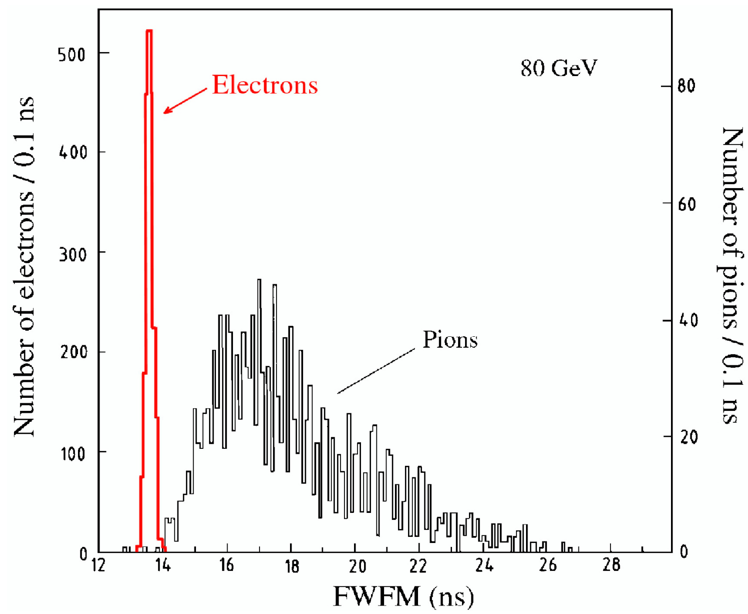

Figure 3: Particle identification in a longitudinally unsegmented calorimeter, on the basis of the time structure of the events. The width of the pulses, measured at 20% of the amplitude provides a clear distinction between electrons and hadrons [9].

respect. Dr. Wigmans has spent most of 2011 in Pisa. TTU has granted him a release of teaching duties in the Spring semester of 2011 to make this possible.

The detector will be modular. Each module contains 4 towers, and is read out by 8 PMTs. Each module is 2.5 m long (10 $\lambda_{\rm int}$), has a cross section of 9.6×9.6 cm^2 and a mass of about 150 kg. The first module was constructed with lead as absorber material, with tools used to build the KLOE calorimeter. A picture of this module is shown in Figure 4. This module was exposed to beam particles at CERN in November 2010, with the purpose to obtain important input for the final design parameters. The analysis has concentrated on the following characteristics:

- The Čerenkov light yield
- The attenuation characteristics of the fibers
- Measurement of the depth of the light production with the DRS information

For the Čerenkov light yield, we measured 32 photoelectrons per GeV deposited energy. For copper absorber, this would translate to about 50 p.e./GeV, because of the suppression of the em response in high-Z absorber material ($e/mip \sim 0.6$). This is still a factor of two less than what we aim for. The main culprit for this difference is Rayleigh scattering at $\lambda < 500$ nm in polystyrene, the core material of the clear fibers used in this module. This feature also limited the attenuation length of the clear fibers to ~ 6 m. For this reason, we have decided to aluminize the upstream ends of the Čerenkov fibers, something that was not foreseen in our original plans. We also decided to use clear fibers based on a PMMA core instead of polystyrene for the detection of Čerenkov light. Bench tests have shown that the effect of a smaller numerical aperture (0.50 instead of 0.72) is more than offset by the decreased light absorption in the short-wavelength

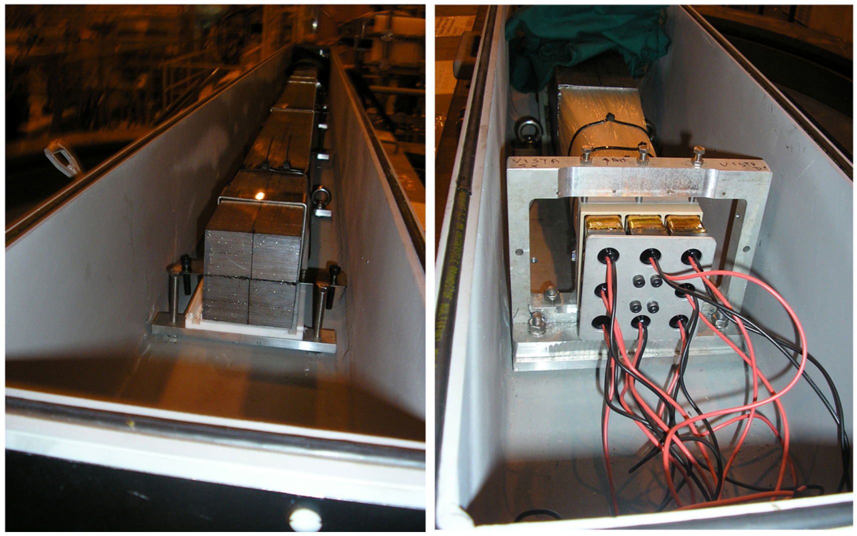

Figure 4: The first new fiber module, recently tested at the H8 beam of the CERN SPS.

region that dominates the Čerenkov spectrum. We have measured attenuation lengths in excess of 20 m for the detector volume in which the light is produced using aluminized Mitsubishi fibers (Figure 5). Because of the mentioned effects (aluminization, Cu absorber, PMMA fibers) we expect the Čerenkov light yield to be close to 100 photoelectrons per GeV in the next module.

The preference for copper as absorber material derives, apart from the higher e/mip value and the associated larger Čerenkov light yield for showers, also from the fact that the mass per $\lambda_{\rm int}^3$ is almost a factor two smaller than for lead. This means that calorimeters, in order to contain hadron showers at the required level, can be much less massive when Cu absorber is used. The fact that $e/mip \sim 0.9$ and not 0.6 as in lead also means much better linearity for hadrons with momenta $\lesssim 5$ GeV/c [10, 11]. Such hadrons form an important component of jets, even at very high energies. It turns out to be non-trivial (*i.e.* expensive) to produce copper profiles with the tolerance level required for our application. For this reason, we maintain lead for the moment as a fall-back solution.

The beam tests of our first (non-aluminized) SuperDREAM prototype module also produced valuable information on the performance of the DRS readout. Figure 6 shows the distribution of the time difference between the PMT signals from 80 GeV electrons measured in the calorimeter and the trigger counters upstream. This difference was obtained by measuring the start of the calorimeter signals with the DRS chip, where the domino wave was started by the trigger signal. We see that a time resolution of slightly more than 1 ns is achieved in this way. This corresponds to a distance of about 20 cm inside the calorimeter.

The first tests of a SuperDREAM module also yielded some results that reveal interesting details about the shower development process. Figure 7 shows an on-line result that could be obtained thanks to the fact that the calorimeter module can be rotated over as much as 90 degrees with respect to the incoming beam particles. The ratio of the Čerenkov and scintillating fiber signals is plotted as a function of the angle of incidence (θ) of the beam particles, 80 GeV electrons in this case, with the fiber direction. The gains of all PMTs were equalized at $\theta = 0°$.

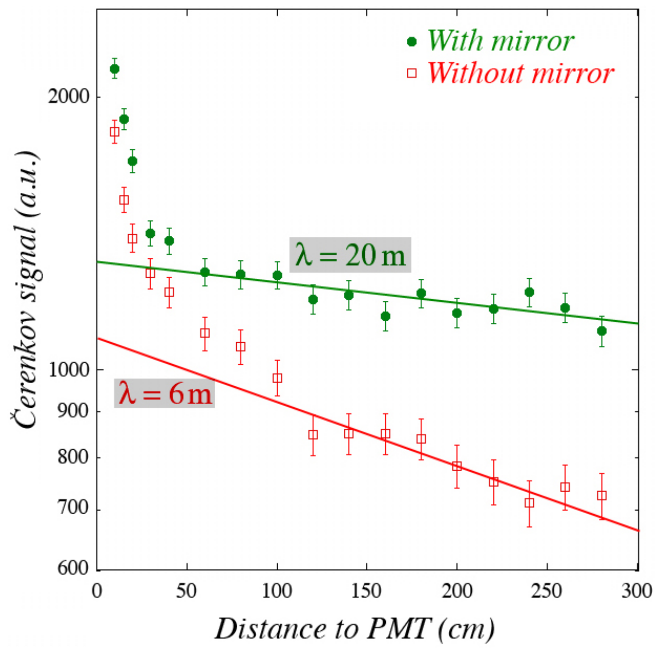

Figure 5: Attenuation characteristics for Čerenkov light in a clear plastic fiber, before and after aluminizing the upstream end. The solid curves, representing an exponential decrease of the measured signal with attenuation lengths of 6m and 20m, respectively, are drawn to guide the eye.

The figure shows that the response ratio is constant up to angles of about $10°$, then increases to reach a maximum at the Čerenkov angle, $\theta_C = 51°$, and decreases at angles beyond this value. The figure also shows that the angular dependence is more significant for the early part of the shower (Tower 4), where the shower particles are more collimated along the beam direction than beyond the shower maximum (Tower 1). This type of measurement has never been performed before. It illustrates that in the early part of the shower, electrons and positrons traveling in (approximately) the same direction as the beam particles form an important contribution to the signals. Beyond the shower maximum, the signal is dominated by particles that have "forgotten" the direction of the incoming particles. As a result, fiber calorimeters with a tower structure which are based on Čerenkov light as the source of the signals can indeed produce good-quality signals from showering particles. When such calorimeters were first proposed, this issue was doubted because it was argued that such calorimeters could only function with the fibers oriented at the Čerenkov angle with respect to the incoming particles [12].

3.2 Near-term plans

In the next two years, we are planning to focus our attention and resources on the following issues:

- Construction of the SuperDREAM fiber calorimeter. The collaboration has currently sufficient resources for the construction of another 15 modules. This would bring the total instrumented mass to about 2.5 tonnes, about half of what is eventually needed to contain

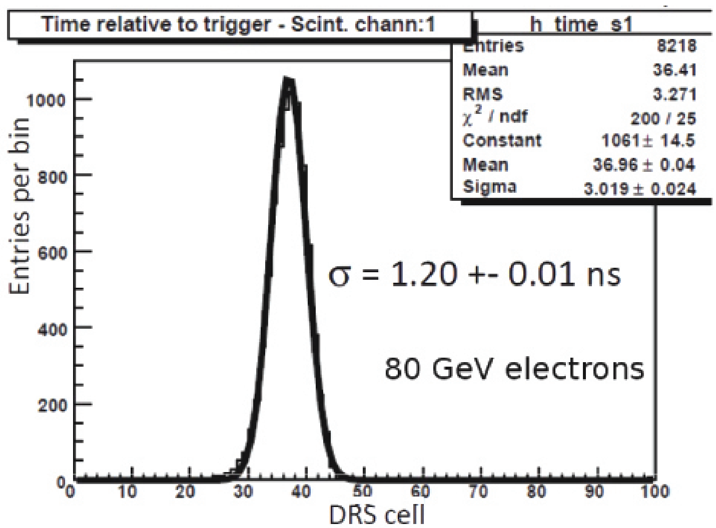

Figure 6: The time resolution for detecting 80 GeV electron showers in the SuperDREAM prototype module with the DRS readout. The readout was triggered by the passage of a beam particle through the upstream trigger counters.

high-energy hadron and jet showers at the required level. We expect to finish the construction of these 15 modules in 2012, and hope to be able to test the assembled detector extensively before the CERN accelerators shut down for a major LHC upgrade in 2013.

- Dealing with shower leakage. We will construct a system of leakage counters, which will surround the SuperDREAM calorimeter. These counters will be specifically sensitive to neutrons, *i.e.* the main component of the shower fraction that escapes detection in the SuperDREAM calorimeter.

- Construction of miscellaneous auxiliary detectors. Another project in which we are going to be involved is the development of a better system for tracking and identifying beam particles. The new beam line (H8) in which future tests are going to be carried out is much less clean than H4, where we worked in the past. We will construct a new fiber-based hodoscope and a veto + preshower detector system which will allow us to define the impact point of the particles with sub-mm precision, and collect clean e, π and μ event samples with 99+% purity.

- The Monte Carlo situation. One of the greatest problems facing experiments that heavily rely on hadron calorimetry is the unsatisfactory state of Monte Carlo simulations of hadron shower development. We have been approached by the GEANT development group at CERN to participate in improving this situation. We will make our expertise, our experimental data and, if at all possible some manpower available for this effort.

3.3 Plans for the longer-term future

Plans for 2013 and beyond include the following:

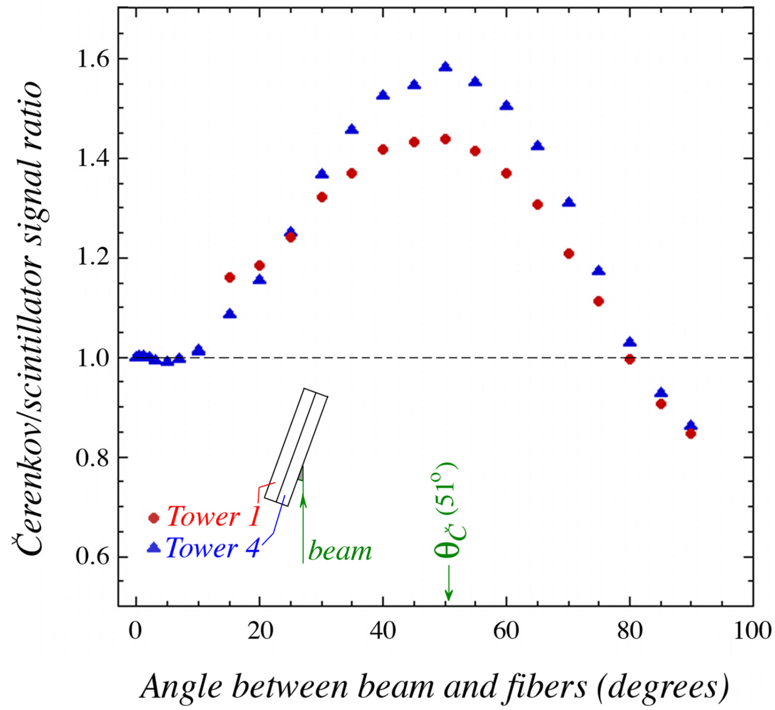

Figure 7: The ratio of the Čerenkov and scintillation signals in the new fiber module, as a function of the angle between the incident 80 GeV electron beam and the fibers. Results are shown for the first part of the shower (Tower 4) and the part beyond the shower maximum (Tower 1). See text for details.

- Completion of the construction of the 5-ton SuperDREAM calorimeter module
- Testing this calorimeter in stand-alone mode, and in combination with an em dual-readout calorimeter consisting of crystals. Currently, we have two crystal matrices that could be used for this purpose, namely a 100-crystal matrix consisting of refurbished BGO crystals from the L3 experiment, and a 7-crystal matrix of molybdenum doped $PbWO_4$ crystals that was specifically developed for our purpose. We are also considering further extending this matrix and/or building a new one out of BSO crystals.
- Development of absorber structures with considerably higher density. This would make it possible to construct more compact calorimeters of this type. Even though the cost of these new structures is likely to be much higher, this may lead to important overall savings. For example, a 10 m long barrel calorimeter with an inner radius of 1 m would encompass an instrumented volume of about 350 m^3. This could be reduced to 180 m^3 if tungsten were used as absorber material instead of copper.
- Studies of projective calorimeter structures based on the DREAM concept. If a calorimeter of the SuperDREAM type was chosen for a 4π experiment, a projective geometry would be required. This poses a number of complications, which are however not unsolvable. In the context of the RD1 and RD25 projects, fully projective fiber calorimeters have been built [13, 14]. We plan to build on the expertise developed in that context.

- Development of an alternative readout system. Splitting the thousands of fibers sticking out of the back, separating them into scintillating and Čerenkov ones and bunching them accordingly is very cumbersome. Moreover, this system takes up valuable space (≈ 50 cm in the detectors we have built so far), and the fiber bunches may sometimes act as antennas, picking up signals that have nothing to do with the ones for which they are intended. For this reason, we have started to look into a readout system based on silicon photomultipliers. The fibers would no longer stick out of the back, but each fiber would be connected to its own individual SiPM, located at the end face of the absorber structure. Given the large surface area that would have to be covered, such a system is at present still prohibitively expensive. However, given the rapid development of this technology, this might change in the years to come. We are in any case planning to test this idea on a modest scale.

4 Requested CERN support

Of course, the plans described in the previous section can only be carried out if our funding agencies provide the means for it. This in turn will depend on the results of future beam tests. However, it will also depend on the perceived status of this project. In that sense, the support from CERN is of crucial importance. Both DOE and INFN would be much more willing to provide funding if this project is embraced by CERN as part of the supported R&D carried out in preparation for future experiments, rather than if it is considered a private hobby of some individuals interested in the generic aspects of calorimetry. We have been told that much by representatives of these organizations.

For this reason, we would like to request that CERN allocate a formal project number to the described research program, *e.g.* RDxx. This would send an unmistakable signal to interested parties that CERN believes that the research carried out in the context of this project addresses important fundamental issues related to future experiments in particle physics, and that CERN supports this research program.

We also ask that CERN make some resources available, particularly in the form of support for carrying out our program of beam tests. A modest account from which crane operations, help from technicians in the workshop of Experimental Hall 887, nuts and bolts from the CERN stores, *etc.* could be covered would be highly appreciated.

References

[1] DREAM Collaboration (Wigmans R) 2010, CERN-SPSC-2010-012/SPSC-M-771.

[2] Akchurin N *et al.* 2009, Nucl. Instr. and Meth. in Phys. Res. **A604**, 512.

[3] Akchurin N *et al.* 2011, Nucl. Instr. and Meth. in Phys. Res. **A638**, 47.

[4] Akchurin N *et al.* 2009, Nucl. Instr. and Meth. in Phys. Res. **A610**, 288.

[5] Akchurin N *et al.* 2011, Nucl. Instr. and Meth. in Phys. Res. **A640**, 91.

[6] Akchurin N *et al.* 2009, Nucl. Instr. and Meth. in Phys. Res. **A598**, 710.

[7] Akchurin N *et al.* 2009, Nucl. Instr. and Meth. in Phys. Res. **A610**, 488.

[8] Akchurin N *et al.* 2008, Nucl. Instr. and Meth. in Phys. Res. **A598**, 422.

[9] Acosta D *et al.* 1991, Nucl. Instr. and Meth. in Phys. Res. **A302**, 36.

[10] Wigmans R 2000, *Calorimetry, Energy Measurement in Particle Physics*, International Series of Monographs on Physics, Vol. 107, Oxford University Press.

[11] Andresen A *et al.* 1990, Nucl. Instr. and Meth. in Phys. Res. **A290**, 95.

[12] Gorodetzky P *et al.* 1995, Nucl. Instr. and Meth. in Phys. Res. **A361**, 161.

[13] Badier J *et al.* 1994, Nucl. Instr. and Meth. in Phys. Res. **A337**, 326.

[14] Anzivino G *et al.* 1995, Nucl. Instr. and Meth. in Phys. Res. **A357**, 350.